Journal of Photochemistry and Photobiology A: Chemistry 205 (2009) 109–115

Contents lists available at ScienceDirect

Journal of Photochemistry and Photobiology A: Chemistry

journal homepage: www.elsevier.com/locate/jphotochem

N, S co-doped and N-doped Degussa P-25 powders with visible light response prepared by mechanical mixing of thiourea and urea. Reactivity towards *E. coli* inactivation and phenol oxidation

J.A. Rengifo-Herrera, J. Kiwi, C. Pulgarin*

SB,ISIC,GGEC, Ecole Polytechnique Fèdéral de Lausanne, 1015 Lausanne, Switzerland

ARTICLE INFO

Article history:
Received 23 October 2008
Received in revised form 23 April 2009
Accepted 24 April 2009
Available online 3 May 2009

Keywords:
Heterogeneous TiO_2 photocatalysis
Visible light response
Nitrogen and sulfur doping
Degussa P-25

ABSTRACT

Degussa P-25 powder was mixed mechanically with thiourea and urea and then annealed during 1 h at 400 °C. Diffuse reflectance spectroscopy (DRS) revealed that treated powders absorb visible light (between 400 and 550 nm) and by Kubelka–Munk relations it was possible to estimate their band-gap energies, being 2.85 and 2.73 eV to thiourea and urea treated powders, respectively. X-ray photoelectron spectroscopy (XPS) showed in the case of thiourea treated P-25, hints of interstitial N-doping and anionic S-doping. On the other hand, P-25 treated with urea showed only the presence of interstitial N-doping. Atomic concentrations measured by XPS showed highest content of N species on TiO_2 surfaces in urea treated P-25 (2.7 at%) while thiourea treated powders presented low concentrations of N and S (0.61 and 0.68 at%, respectively). Specific surface area (SSA) was measured by BET method, obtaining values of 52 and 46 $m^2\,g^{-1}$ for undoped P-25 and undoped P-25 annealed at 400 °C during 1 h. N, S co-doped and N-doped P-25 showed SSA of 42 and 40 $m^2\,g^{-1}$, respectively. We suggest that probably •OH radical is not directly involved in oxidative processes taking place when N, S co-doped Degussa P-25 was exposed to visible light.

1. Introduction

In the last 25 years, heterogeneous photocatalysis over TiO_2 has generated a growing interest as a promissory technology to degrade chemical substances and inactivate pathogen cells in aqueous solution, since titanium dioxide presents suitable features such as: low cost, ready commercial availability [1,2].

Degussa P-25 (mix of 70% anatase and 30% rutile) is the commercial TiO_2 powder with the highest photocatalytic activity and most often used as a standard photocatalyst. Some authors have argued that mixed-phase materials such as Degussa P-25 can present low e^-/h^+ recombination since electrons photo-produced on anatase phase can be transfer to lower energy rutile electron trapping sites [3]. However, recently Hurum et al. [4] have proposed by electronic paramagnetic resonance (EPR) measurements that exist an interwoven between anatase and rutile crystallites facilitating the efficient electron transfer at the anatase/rutile interface. Moreover, it could be possible the electron transfer from rutile phase to surface trapping sites on the anatase.

However, one of the main disadvantages of heterogeneous photocatalysis over TiO_2 is their incapacity to absorb visible light, since titania photocatalyst absorbs only UV light that is 3–4% of the total solar radiation hitting the terrestrial surface. For this reason, the search of materials based on TiO_2 with visible light response has gained attention in the last years [5] and new materials of anatase or rutile powders doped with lowest quantities of N or/and S and C have been reported able to absorb visible light [6,7].

N- and S-doping creates localized N or S states within the TiO_2 band-gap. The electron promotion from these localized states would be responsible of its visible light absorption [8,9].

The literature reports different techniques to prepare N- or S-doped TiO_2. It is most often mentioned the preparation of N- and S-doped TiO_2 via hydrolytic processes such as sol–gel giving mainly N-doped or S-doped anatase phase [10–12].

Also N-doped Degussa P-25 powder was obtained when the titania powder is treated under NH_3/Ar flow at different temperatures between 500 and 600 °C [13,14].

S-doping P-25 was prepared by ball-milling with thiourea and then annealing at 400 and 600 °C during 30 min or 2 h under vacuum atmospheres has also been reported [15].

N- or S-doped Degussa P-25 powders have been tested to in the degradation of methylene blue and phenol under visible light [13,14].

Hereby, we report the preparation of N, S co-doped TiO_2 P-25 and N-doped TiO_2 P-25 by mechanical mixing of thiourea and urea, respectively. N, S co-doped Degussa P-25 and N-doped

* Corresponding author. Tel.: +41 21 693 47 20; fax: +41 21 693 6161.
E-mail address: cesar.pulgarin@epfl.ch (C. Pulgarin).

1010-6030/$ – see front matter © 2009 Elsevier B.V. All rights reserved.
doi:10.1016/j.jphotochem.2009.04.015

Degussa P-25 powders were characterized by Diffuse Reflectance Spectroscopy (DRS), X-ray photoelectron spectroscopy (XPS) BET. Photocatalytic activities of these powders were tested using phenol and *Escherichia coli* (*E. coli*) cells under UV (320–380 nm) and visible light (400–500 nm).

2. Experimental

2.1. Materials

Commercial powder of Degussa P-25 (70% anatase, 30% rutile and specific surface area (SSA) of 50 g m^{-2}) was used as obtained from Degussa AG. Bidistilled Milli-Q water was used throughout this study. Thiourea, urea and phenol were purchased from Sigma–Aldrich (99%).

2.2. Preparation of doped Degussa P-25

Doped TiO_2 was prepared by manual grinding of thiourea or urea with TiO_2 in a 4:1 ratio during 1 h. The materials were annealed under air atmosphere during 1 h at 400 °C with a heating rate of 10 °C per minute and cooled at room temperature. After heating the materials were washed with Milli-Q water three times and dry at 70 °C and then crushed in an agate mortar into a fine powder before use.

2.3. Powder characterization

2.3.1. Diffuse reflectance UV–vis spectroscopy (DRS)

DRS spectra of TiO_2 powders were measured with a Varian Cary 1E spectrophotometer equipped with a diffuse reflectance accessory. The Kubelka–Munk relation [16] was used to transform the reflectance data into absorption spectra. A Kodak analytical standard white reflectance coating was used as reference. Diffuse reflectance can be related to the absorbance by the K/S ratio using the Kubelka–Munk relations ($F(R_\infty)$) (Eq. (1)), where the scattering is noted as S and reflectance is noted as R. The reflectance relates to the absorption coefficient α (K/S) and this is proportional to absorbance K (Eq. (1))

$$\frac{K}{S} = \frac{(1-R_\infty)^2}{2R_\infty} \equiv F(R_\infty) \quad (1)$$

2.3.2. X-ray photoelectron spectroscopy (XPS)

XPS analyses were carried out on a XPS Analyzer Kratos model Axis Ultra with a monochromatic AlKα and charge neutralizer.

The deconvolution software program was provided by Kratos the manufacturer of the XPS instrument.

All the binding energies were referenced to the C 1s peak at 285 eV of adventitious carbon. Powder samples were prepared by deposition of catalyst on carbon type stuck to sample holder. The powder samples were analyzed with very large spot with dimension 0.3 mm × 0.7 mm. Therefore it is assumed that the recorded spectrum is characteristic for average particles. Using a large spot we improved significantly the signal/noise ratio.

The atomic concentrations were determined with an increased sensitivity factor because in general the signal/noise ratio is weak. This analysis was carried out: (a) taking a larger area, (b) the signal accumulation time was increased and (c) the elements analyzed like N did not have a weak sensitivity. The detection limit was not 0.1 at% but 0.03 at%.

2.3.3. Specific surface area (SSA)

Specific surface area (SSA) was measured using nitrogen adsorption–desorption at 77 K via a Sorptomatic 1990 instrument (Carlo Erba) and calculated using the Brunauer–Emmet–Teller (BET) method.

2.4. Photocatalytic activity testing

Cylindrical Pyrex bottles (50 ml) were used, a TiO_2 concentration of 1.0 g l^{-1} was selected since in previous studies carried out for our group, it was found this concentration as the optimal for the experimental set-up used [17,18]. Oxygen (present in the air) was used as electron acceptor. The suspension was kept under magnetic stirring at 500 rpm and it was irradiated by five Black light lamps Phillips TLD 18W (emission spectra: 330–400 nm and UV intensity between 300 and 400 nm: 38 W m^{-2}) and five fluorescent lamps Phillips TLD-18W blue (emission spectra: 400–500 nm. UV intensity: 0.1 W m^{-2} and intensity between 290 and 1100 nm: 60 W m^{-2}). The radiant flux was monitored with a Kipp & Zonen (CM3) power meter (Omni instruments Ltd., Dundee, UK).

Temperature of the experiments was never superior to 38 °C. Samples were periodically collected to follow the reaction kinetics. Results represent the average of three experimental runs and their standard deviations were equal or lower than 15% for microbiological analysis and 6% for HPLC analysis.

2.4.1. Bacterial inactivation

Photocatalytic activity in bacterial inactivation was measured by sampling from the photoreactor an *E. coli* strain K12 MG 1655. Before the experiment, bacteria were inoculated into nutrient broth (Oxoid no. 2, Switzerland) and grown overnight at 37 °C. During the stationary growth phase, bacteria cells were harvested by centrifugation at 5000 rpm for 10 min at 4 °C. The bacterial pellet was then washed three times with a saline solution (8 g l^{-1} NaCl and 0.8 g l^{-1} KCl in Milli-Q water, pH 7 by addition of HCl or NaOH). A suitable cell concentration (10^4 colony forming units per milliliter (CFU ml^{-1})) was inoculated in the reactor's saline solution

Then, the inoculated Pyrex bottles with the catalyst added were illuminated during 2 h and samples (1.0 ml) were taken at different time intervals. Serial dilutions were performed in saline solution and 100 μl volumes were inoculated in a plate count agar (PCA, Merck, Germany) growth medium. The number of colonies was counted 24 h after incubation at 37 °C. Control experiments (*E. coli* and UV or visible light without catalyst) and (*E. coli* + catalyst without light) were also performed.

2.4.2. Phenol photocatalytic oxidation

Phenol solution containing 1×10^{-4} M was added to the Pyrex glass reactors. Samples were taken and filtered by 0.2 μm membranes. Phenol oxidation was followed by HPLC (Hewlett-Packard series 1100) with a reverse phase Spherisorb silica column (Macherey-Nageland). As mobile phase was used acetonitrile:water (60:40). Phenol and p-benzoquinone detection was carried out by Diode Array Detector (DAD) at 220 and 244 nm, respectively. While the HPLC experiments were carried out, it was found the retention times of the peaks detected were shifted. In order to clarify this fact, the retention times were contrasted with internal standards of phenol and p-benzoquinone and their absorption spectra were recorded using the Diode Array Detector (DAD).

3. Results and discussion

3.1. Powders characterization

3.1.1. Diffuse reflectance spectroscopy (DRS) and Kubelka–Munk relations

Fig. 1 shows the K/S ratio vs. wavelength. Degussa P-25 shows absorption <410 nm. Degussa P-25 treated with urea and thiourea showed the absorption corresponding to pure Degussa P-25 but

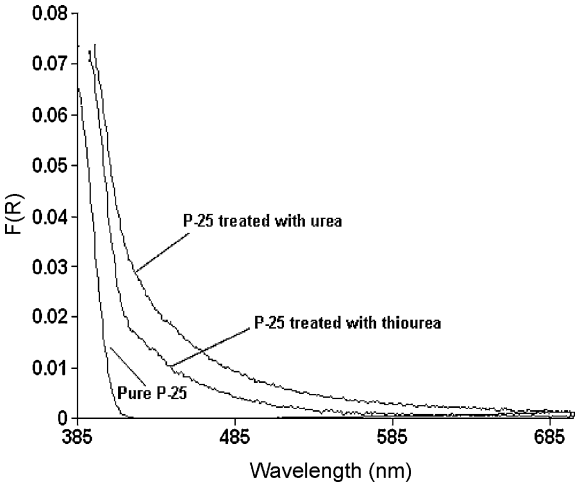

Fig. 1. UV–vis spectra of pure P-25, urea treated P-25 and thiourea treated P-25.

also absorption between 400 and 550 nm being the absorption of powders doped with urea more intense.

By Kubelka–Munk relations we estimated the band-gap energy of doped powders. Band-gap energy of pure Degussa P-25 was estimate to be 3.10 eV close to the value of 3.15 eV reported in the literature [3]. Thiourea and urea doped Degussa P-25 powders showed a reduced band-gap with values of 2.83 and 2.73 eV, respectively.

3.1.2. X-ray photoelectron spectroscopy measurements of thiourea doped P-25

XPS measurements were carried out to detect the surface species on the titania surface responsible for the visible absorption. Degussa P-25 did not reveal any presence of N or S impurities.

Thiourea doped powder shows the presence of N 1s, S 2p and C 1s XPS peaks (Fig. 2). Deconvolution of N 1s peak revealed the presence of two peaks with binding energies (BEs) at 399 and 401 eV. Recently, in the literature, there has been a controversy about the assignation of N 1s peaks in N-doped TiO_2. Asahi et al. [19] and other authors [20,21] claimed that N- can substitute oxygen atoms on the titania surface producing an XPS-N 1s peak localized at 397 eV. This specie would be the responsible of N-doped TiO_2 and visible absorption. However, on the other hand, Yates et al. [22] and Gopinath et al. [23] have suggested that the peaks at 399 eV and BE > 400 eV were due to interstitial N-doping and/or the formation of N–O–Ti species.

In this study we suggest that Degussa P-25 powders doped with thiourea present interstitial N-doping since the presence of the N 1s peak at 397 eV was not observed.

Regarding the S 2p peak deconvoluted, it was possible to detect several S 2p peaks, indicating that the sulfur is present on the TiO_2 surface in different oxidation states. For instance, it was detected a peak at 168.7 and 169.9 eV corresponding to S^{6+}. In the literature, this peak is often assigned to presence of SO_4^{2-} ions on the titania surface [15,23,24]. The peak at 164.2 eV could be due to the presence of SO_3^- [15]. Finally a peak at 163 eV was also detected and has been assigned to Ti–S bonds, due to anionic S-doped TiO_2. In this case an oxygen atom is substituted by an S atom [25,26].

The C 1s peaks revealed only the presence of adventitious carbon (peak at 284.5 and 285.5 eV) due to sample contamination. It was also possible to detect the presence of carbonates on the titania surface (peak at 288.5 eV) formed during the thermal decomposition of the thiourea. It was not found the presence of XPS peaks of anionic C-doped TiO_2 localized at BE of 282 eV [27].

Table 1
Atomic concentration in (at%) and specific surface area (SSA) of doped powders.

Powder	N 1s (at%)	S 2s (at%)	SSA ($m^2\ g^{-1}$)
Undoped P-25	0.0	0.0	52
N, S co-doped P-25	0.61	0.66	46
N-doped P-25	2.7	0.0	40

In summary, powders of Degussa P-25 mixed with thiourea and annealed at 400 °C during 1 h produced N and S co-doped TiO_2 with visible light absorption.

3.1.3. X-ray photoelectron spectroscopy measurements of urea doped P-25

Fig. 3 shows the XPS spectra of Degussa P-25 powders treated with urea. It was possible to observe the presence of N 1s and C 1s peaks.

By deconvolution, three N 1s peaks were found; two at 399 and other at 401 eV. These peaks are assigned to interstitial N-doping and/or the formation of N–O–Ti species.

C 1s peaks did not reveal the presence of C-doped TiO_2 (absence of peak at 282 eV). It was only found the presence of adventitious carbon (peak with BE at 285 and 286 eV) and carbonates (peak with BE at 288 eV) [28–30]. With this evidence, we can suggest that Degussa P-25 powders mixed mechanically with urea and then annealed at 400 °C during 1 h produced substitutional N-doped TiO_2.

Theoretical studies have suggested that the N or S-doping of TiO_2 can generate localized N or S states within the band-gap and it is from these localized states where the electronic promotion to the conduction band under visible light takes place [8,9].

Moreover the content of N and S (in atomic concentration %) in the N, S co-doped and N-doped powders is showed in Table 1. N-doped TiO_2 presents higher N concentration than the N, S co-doped TiO_2, and this could explain the higher absorption intensity of visible light (Fig. 1). Irie et al. [31] have reported that when N concentration increases the absorption intensity of N-doped TiO_2 also increases.

3.1.4. Specific surface area measurements

BET experiments were carried out in order to determine the specific surface area (SSA) of the materials. Doped materials present a decreasing in their surface area. The starting material (pure Degussa P-25) had a SSA around of 52 $m^2\ g^{-1}$, and after annealing at 400 °C during 1 h, the SSA decreased to 46 $m^2\ g^{-1}$. N, S co-doped TiO_2 showed an SSA of 42 $m^2\ g^{-1}$. N-doped powder presented an SSA of 40 $m^2\ g^{-1}$.

3.2. Photocatalytic activity

3.2.1. Photocatalytic activity of N, S co-doped TiO_2 and N-doped TiO_2 under UV light exposure

Fig. 4a shows the results of *E. coli* inactivation obtained with pure P-25, pure P-25 annealed at 400 °C, N, S co-doped P-25 and N-doped P-25 under UV illumination. It can be observed that annealing and N- or S-doping of Degussa P-25 powders produced a detrimental effect on the photocatalytic *E. coli* inactivation being stronger on N-doped powders.

When phenol oxidation was tested under UV illumination (Fig. 4b), the same pattern was observed for *E. coli* inactivation. p-benzoquinone was the main by-product generated during the first steps of phenol oxidation (Fig. 5a and b) either with Degussa P-25 and doped samples of this powder.

It is well known the first step of phenol oxidation is the nucleophilic attack of •OH radical on the aromatic moiety producing hydroquinone or p-benzoquinone as main by-products and then

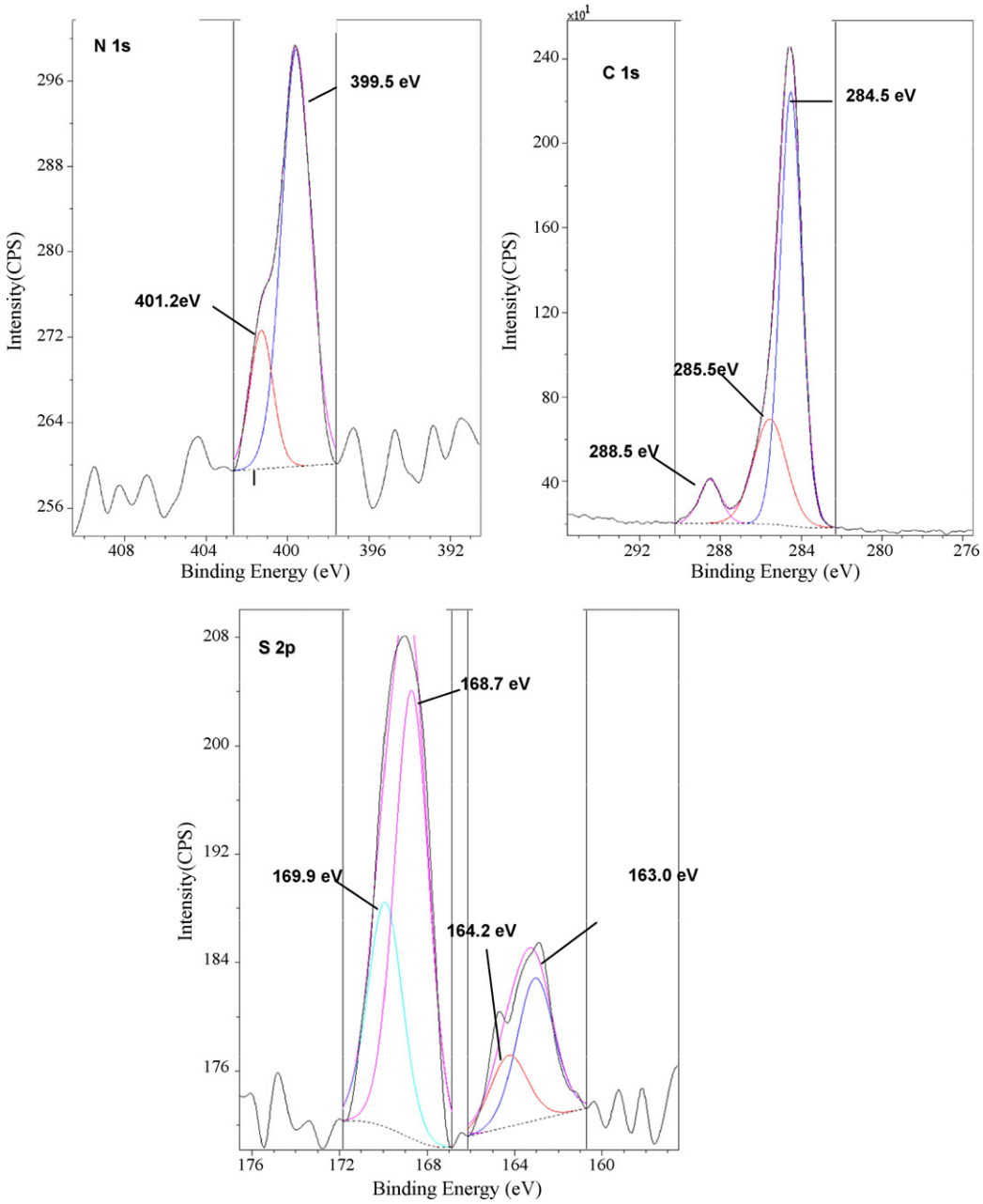

Fig. 2. XPS of thiourea doped P-25 powders.

the aromatic ring when broken leads to aliphatic acids [32,33]. This suggests that under UV irradiation the classical mechanism of photocatalysis on TiO_2 is involved where the main oxidative specie responsible of *E. coli* inactivation and phenol oxidation produced during UV illumination is the •OH radical generated by direct h_{VB}^+ oxidation of H_2O or OH^- ions (Scheme 1).

During the annealing of the TiO_2 powder sintering occurs resulting in a particle size increase. This effect favors the recombination processes since electrons and holes cannot easily reach the surface within their lifetimes limiting the formation of surface ROS [34]. The BET measurements show that when doped TiO_2 P-25 powders were annealed the particle size increases and the BET of the powders decrease.

Other effect linked to annealing of titania powders is the de-hydroxylation of their surfaces. This process affect also the photocatalytic activity since hydroxyl groups act as charges carriers traps avoiding charge recombination and producing reactive oxidative species (ROS) responsible for the bacterial inactivation and intervening in the oxidation of chemical substances [35].

Concentration of N or S impurities could also negatively affect the photocatalytic activity of doped powders since some authors have reported that the presence of N or S impurities can act as recombination centers [28]. N-doped P-25 showed highest N atomic concentrations (around 2.7 at%) indicating that the recombination processes could be favored. For N, S co-doped P-25, where the atomic concentrations of N and S were lowest (see Table 1) this effect is less important.

3.2.2. *Photocatalytic activity of N, S co-doped TiO_2 and N-doped TiO_2 under visible light exposure*

In Fig. 1 it was demonstrated that N, S co-doped and N-doped P-25 powders absorb visible light. The photocatalytic activity is shown for λ between 400 and 500 nm. Fig. 6 shows the photocatalytic *E. coli* inactivation under visible light. N, S co-doped

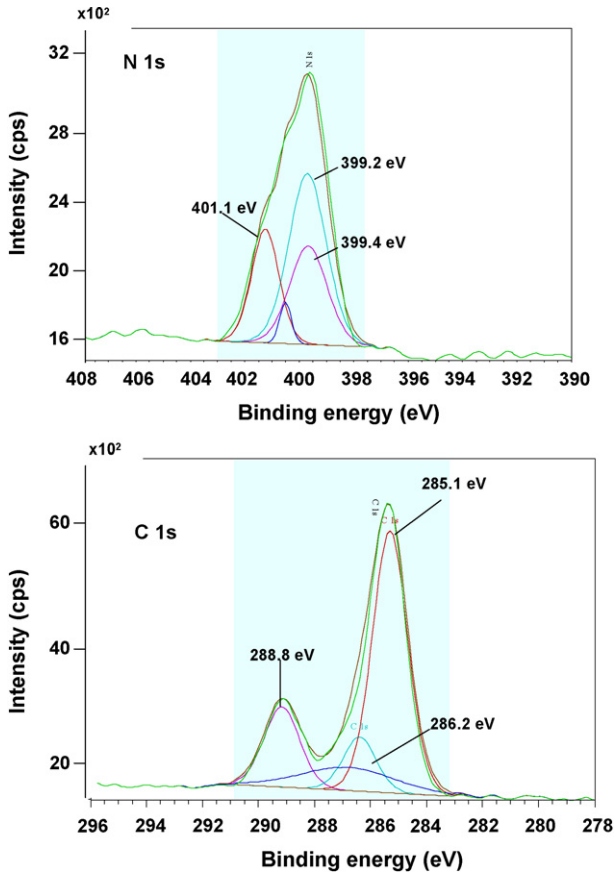

Fig. 3. XPS of urea treated P-25 powders.

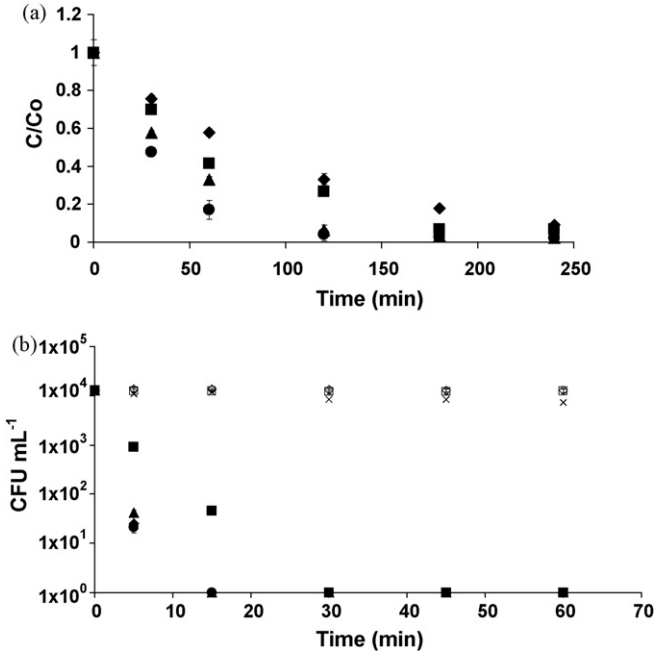

Fig. 4. Photocatalytic *E. coli* inactivation (a) and phenol oxidation (b) under UV light irradiation. (●) Pure Degussa P-25, (▲) pure Degussa P-25 annealed at 400 °C, (♦) N, S co-doped P-25 and (■) N-doped P-25, (◊) N, S co-doped P-25 in the dark, (□) N-doped P-25 in the dark, (×) UV exposure without catalyst. No phenol adsorption and phenol degradation by UV light were observed. pH 7.0, UV intensity 30 W m^{-2}.

Degussa P-25 is shown to be the powder with highest photocatalytic activity.

In spite of N-doped Degussa P-25 showing highest visible absorption, its photocatalytic activity was lowest probably due to its high N concentration acting as recombination centers. Pure Degussa P-25 and pure Degussa P-25 annealed at 400 °C were also active under visible illumination. Hurum et al. [4] found that under illumination at $\lambda > 400$ nm generation of pair e^-/h^+ seems to be possible since rutile (with $E_{bg} = 3.0$ eV) can absorb $\lambda < 410$ nm.

However, no phenol degradation was found when doped and undoped Degussa P-25 powders were illuminated by visible light (data not showed). Moreover, we demonstrated in a previous work, that bacteria seem to be more sensible to the ROS generated on anatase TiO_2 upon visible light exposition than chemical compounds [36]. Under visible light we observed a strong *E. coli* inactivation with N, S co-doped P-25. No phenol oxidation was found suggesting probably other photocatalytic mechanism acting.

Mitoraj et al. [37] reported that C-doped TiO_2 and TiO_2 modified with platinum (IV) chloride complexes with visible response showed bacterial inactivation under visible light probably due to an indirect pathway to generate •OH radicals from the reduction of molecular oxygen by e^-_{CB}. This reduction produces $•O_2^-$ that quickly disproportionates generating H_2O_2. This hydrogen peroxide is reduced by e^-_{CB} to produce •OH radicals.

Furthermore, Mrowetz et al. [38] suggest the lack of •OH radicals when N-doped TiO_2 was illuminated under visible light. They suggest that the electron promoted to the conduction band is the only charge carrier capable to induce redox reactions in the N-doped TiO_2 surfaces. Livraghi et al. [39] proposes the e^-_{cb} is the species which participates in the surface redox reactions.

Experimental results obtained by time-resolved diffuse reflectance spectroscopy by Tachikawa et al. [40] showed that the holes photogenerated in C- and S-doped TiO_2 under UV-light can be easily trapped on the surface and then react with the adsorbed organic compounds. In contrast, under visible irradiation the holes generated have a lower redox potential not suitable for the

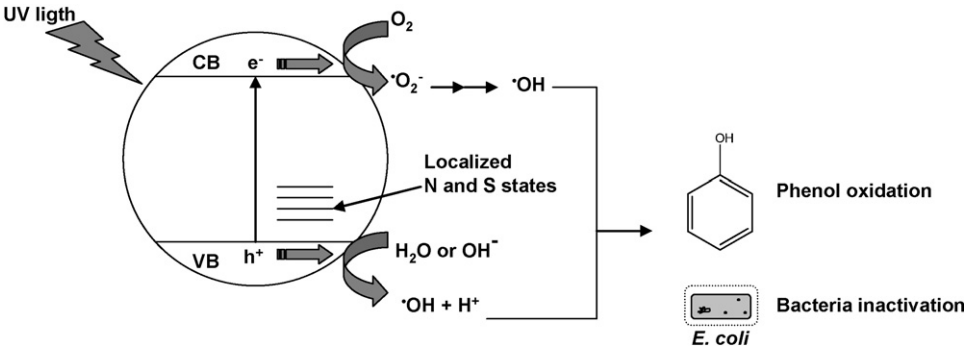

Scheme 1. Photocatalytic *E. coli* inactivation and phenol oxidation carried out by •OH radicals under UV irradiation on N, S co-doped P-25.

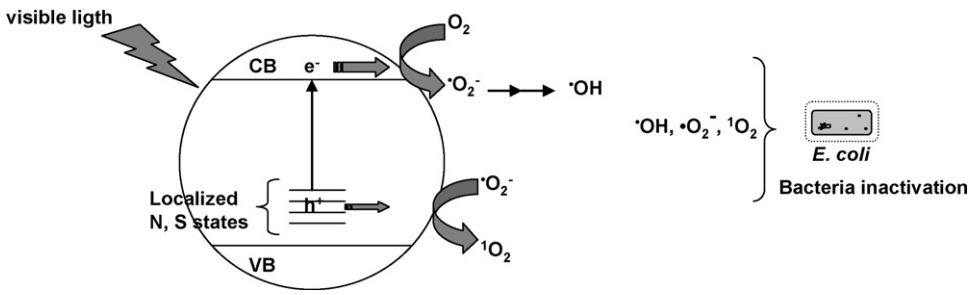

Scheme 2. Photocatalytic *E. coli* inactivation carried out by •OH radicals produced indirectly, superoxide radical and single oxygen under visible light irradiation on N, S co-doped P-25.

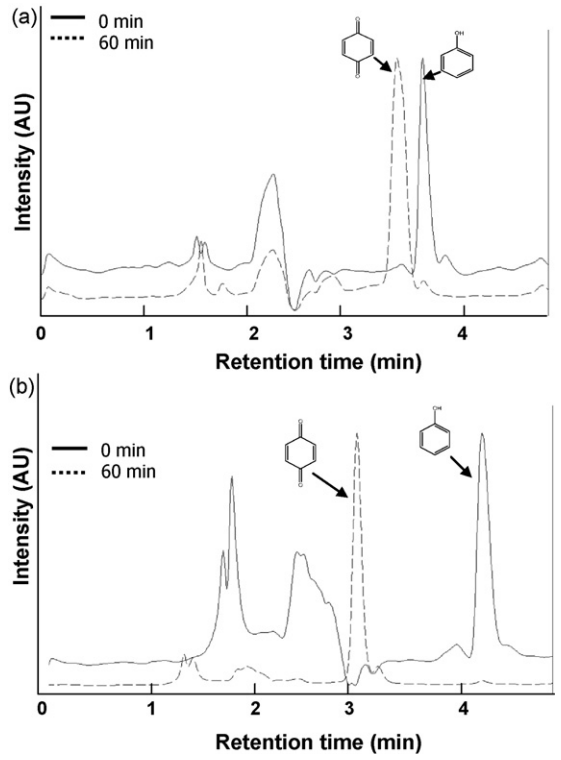

Fig. 5. Chromatograms obtained with DAD at 244 nm showing the formation of p-benzoquinone after 60 min of UV illumination. (a) Pure P-25 and (b) N, S co-doped P-25.

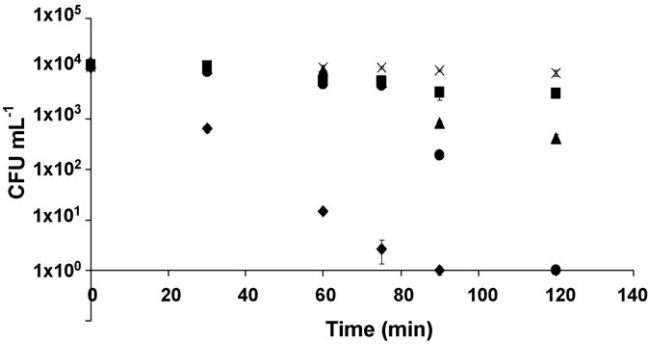

Fig. 6. Photocatalytic *E. coli* inactivation under visible light irradiation. (●) Pure Degussa P-25, (▲) pure Degussa P-25 annealed at 400 °C, (♦) N, S co-doped P-25 and (■) N-doped P-25, (×) visible light exposure without catalyst. pH 7.0, UV intensity 0.1 W m^{-2} and visible light intensity: 60 W m^{-2}.

oxidation of the organic compound in solution as it is the case of Degussa P-25 TiO_2. Recently, we have proposed that through the ESR spin trapping measurements the formation of singlet oxygen is thermodynamically favored under visible light irradiation through a mechanism that implicates the generation of the superoxide radical by the e_{cb}^- reduction of the molecular oxygen on N, S co-doped TKP 102 powders [41].

So, in this work, we suggest that under visible irradiation, the electronic promotion in N, S co-doped P-25 yield holes in the N and S localized states within the band-gap having a lower oxidative potential than the oxidative radicals produced by Degussa P-25 undoped powder. The following event is the transfer of CB electrons to molecular oxygen producing superoxide radical toxic to bacteria [42].

It is also well known that the superoxide radical at pH > 4.8 is protonated producing •OOH and then the main via of •OOH inactivation is its disproportion to H_2O_2. The H_2O_2 participate in reduction reactions producing •OH radicals [43,44].

$$^{\bullet}O_2^- + H^+ \rightarrow {}^{\bullet}O_2H \quad (pK_a = 4.69) \tag{2}$$

$$^{\bullet}O_2H + {}^{\bullet}O_2^- + H^+ \rightarrow H_2O_2 + O_2 \tag{3}$$

$$^{\bullet}O_2H + {}^{\bullet}O_2H \rightarrow H_2O_2 + O_2 \tag{4}$$

$$^{\bullet}O_2^- + {}^{\bullet}O_2^- + H^+ \rightarrow H_2O_2 + O_2 \tag{5}$$

$$H_2O_2 + e^-{}_{CB} \rightarrow {}^{\bullet}OH + OH^- \tag{6}$$

Furthermore, it is possible that during the visible illumination the radical $^{\bullet}O_2^-$ produced by molecular oxygen reduction may also be oxidized by holes produced from the N and S localized states yielding singlet oxygen. It has been reported the production of singlet oxygen on Degussa P-25 TiO_2 under UV illumination [45]. The oxidation of $^{\bullet}O_2^-$ to produce singlet oxygen has a redox potential of 0.34 V vs. NHE [44]. The formation of singlet oxygen through superoxide radical oxidation by localized N or S holes, it seems thermodynamically probable.

In summary, the visible light *E. coli* inactivation obtained by N, S co-doped P-25 powders could be carried out by electrons promoted from the localized N or S states on the band-gap to the conduction band. This electron could participate in charge transfer reactions, mainly molecular oxygen reduction, producing directly $^{\bullet}O_2^-$, indirectly produced •OH radicals and singlet oxygen $^1O_2$ as ROS toxic to the cells (Scheme 2).

4. Conclusions

N, S co-doped and N-doped P-25 powders with visible light response were prepared by mechanical mixing with thiourea and urea respectively and then annealing at 400 °C for 1 h.

Annealing and highest doping concentration cause a detrimental effect on the photocatalytic activity towards *E. coli* and phenol under

UV exposition. However, N, S co-doped P-25 showed a strong *E. coli* inactivation under visible light, while phenol was not oxidized. With these results, we suggest that the electron photo-promoted from the localized N and S states is the charge carrier responsible of the ROS formation. The main oxidative species are suggested to be the superoxide radical ($^{\bullet}O_2^-$) and the singlet oxygen ($^1O_2$), both species toxic to microorganisms but probably innocuous to phenol under visible light irradiation of doped Degussa P-25 TiO_2.

Acknowledgements

The authors thank the Swiss Agency for Development and Cooperation and Cooperation@EPFL for its support to BIOSOLARDETOX project, the Cost Action 540 (PHONASUM) from the Secretariat d'Etat à l'éducation et à la recherche SER, Confédération Suisse, Project No. C06.0074, Professor J.-E. Moser and J. Teuscher from the Photochemical Dynamics Group (EPFL-Switzerland) for their help in the recording of DRS spectra, N. Xanthopoulos from Surface analysis laboratory-EPFL for kindly recording the XPS spectra. E. Casali for kindly recording the BET measurements and N.C. Castillo for his help and comments. J.A. Rengifo-Herrera is very grateful to M.L. Molina for her continuous encouragement.

References

[1] M.R. Hoffmann, S.T. Martin, W. Choi, D.W. Bahnemann, Environmental applications of semiconductor photocatalysis, Chem. Rev. 95 (1995) 69–169.
[2] A.L. Linsebigler, G. Lu, J.T. Yates, Photocatalysis on TiO_2 surfaces: principles, mechanisms, and selected results, Chem. Rev. 95 (1995) 735–758.
[3] R.I. Bickley, T. Gonzales-Carreno, J.S. Lees, L. Palmisano, R.J.D. Tilley, A structural investigation of titanium dioxide photocatalysts, J. Solid State Chem. 92 (1991) 178–190.
[4] D.C. Hurum, A.G. Agrios, K.A. Gray, T. Rajh, M.C. Thurnauer, Explaining the enhanced photocatalytic activity of Degussa P25 mixed-phase TiO_2 using EPR, J. Phys. Chem. B 107 (2003) 4545–4549.
[5] D. Chatterjee, S. Dasgupta, Visible light induced photocatalytic degradation of organic pollutants, J. Photochem. Photobiol. C 6 (2005) 186–205.
[6] T.L. Thompson, J.T. Yates, Surface Science studies of the photoactivation of TiO_2-new photochemical processes, Chem. Rev. 106 (2006) 4428–4453.
[7] A.V. Emeline, V.N. Kuznetsov, V.K. Rybchuk, N. Serpone, Visible-light active titania photocatalysts: the case of N-doped TiO_2s-properties and some fundamental issues, Int. J. Photoenergy (2008), doi:10.1155/2008/258394.
[8] S. Livraghi, A.M. Votta, M.C. Paganini, E. Giamello, The nature of paramagnetic species in nitrogen doped TiO_2 active in visible light photocatalysis, Chem. Commun. (2005) 498–500.
[9] T. Umebayashi, T. Yamaki, H. Itoh, K. Asai, Band gap narrowing of titanium dioxide by sulphur doping, Appl. Phys. Lett. 81 (2002) 454–456.
[10] S. Sato, R. Nakamura, S. Abe, Visible-light sensitization of TiO_2 photocatalyst by wet-method N doping, Appl. Catal. A 284 (2005) 131–137.
[11] Y. Cong, J. Zhang, F. Chen, M. Anpo, Synthesis and characterization of nitrogen-doped TiO_2 nanophotocatalyst with high visible light activity, J. Phys. Chem. C 111 (2007) 6976–6982.
[12] T. Ohno, M. Akiyoshi, T. Umebayashi, K. Asai, T. Mitsui, M. Matsamura, Preparation of S-doped TiO_2 photocatalysts and their photocatalytic activities under visible light, Appl. Catal. A 265 (2004) 115–121.
[13] W. Yan, Z. Jiwei, J. Zhen Shen, W. Zhishen, Z. Shunli, Visible light photocatalytic decoloration of methylene blue on novel N-doped TiO_2, Chin. Sci. Bull. 52 (2007) 2157–2160.
[14] X. Fang, Z. Quinglin Chen, H. Ji, X. Gao, Dependence of nitrogen doping on TiO_2 precursor annealed under NH_3 flow, J. Solid State Chem. 180 (2007) 1325–1332.
[15] L.K. Randeniya, A.B. Murphy, I.C. Plumb, A study of S-doped TiO_2 for photoelectrochemical hydrogen generation from water, J. Mater. Sci. 43 (2008) 1389–1399.
[16] P. Kubelka, F. Munk, Zei. Tech. Phys. 12 (1931) 593–601.
[17] A.G. Rincon, C. Pulgarin, Photocatalytic inactivation of *E. coli*: effect of (continuous-intermittent) light intensity and (suspended-fixed) TiO_2 concentration, Appl. Catal. B 44 (2003) 263–284.
[18] D. Gumy, S.A. Giraldo, J. Rengifo, C. Pulgarin, Effect of suspended TiO_2 physicochemical characteristics on benzene derivatives photocatalytic degradation, Appl. Catal. B 78 (2008) 19–29.
[19] R. Asahi, T. Morikawa, T. Ohwaki, K. Aoki, Y. Taga, Visible-light photocatalysis in nitrogen-doped titanium oxides, Science 293 (2001) 269–271.
[20] A. Nambu, J. Graciani, J.A. Rodriguez, Q. Wu, E. Fujita, J.J. Fernandez-Sanz, N-doping of TiO_2 (1 1 0): photoemission and density-functional studies, J. Chem. Phys. 125 (2006) 094706-1–194706-8.
[21] O. Diwald, T.L. Thompson, E.G. Goralski, S.D. Walck, J.T. Yates, The effect on nitrogen ion implantation on the photoactivity of TiO_2 rutile single crystals, J. Phys. Chem. B 108 (2004) 52–57.
[22] O. Diwald, T.L. Thompson, E.G. Goralski, S.D. Walck, J.T. Yates, Photochemical activity of nitrogen-doped rutile TiO_2 (1 1 1) in visible light, J. Phys. Chem. B 108 (2004) 6004–6008.
[23] M. Sathish, B. Viswanathan, R.P. Viswanath, C.S. Gopinath, Chem. Mater. 17 (2005) 6349–6353.
[24] G. Colón, H. Hidalgo, G. Munuera, I. Ferino, M.G. Cutrufello, J.A. Navío, Structural and surface approach to the enhanced photocatalytic activity of sulfated TiO_2 photocatalyst, Appl. Catal. B 63 (2006) 45–59.
[25] T. Umebayashi, T. Yamaki, A. Yamamoto, A. Miyashita, S. Tanaka, T. Sumita, K. Asai, Sulfur-doping of rutile-titanium dioxide by ion implantation: photocurrent spectroscopy and first-principles band calculation studies, J. Appl. Phys. 93 (2003) 5156–5160.
[26] E.L.D. Hebenstreit, W. Hebenstreit, U. Diebold, Structures of sulfur on TiO_2 (1 1 0) determined by scanning tunneling microscopy X-ray photoelectron spectroscopy and low energy electron diffraction, Surf. Sci. 470 (2001) 347–360.
[27] R.W. Matthews, S.R. McEvoy, Photocatalytic degradation of phenol in the presence of near-UV illuminated titanium dioxide, J. Photochem. Photobiol. A 64 (1992) 231–246.
[28] H. Sun, Y. Bai, Y. Cheng, W. Jin, N. Xu, Preparation and characterization of visible-light-driven carbon–sulfur-codoped TiO_2 photocatalysts, Ind. Eng. Chem. Res. 45 (2004) 4971–4976.
[29] J. Yang, H. Bai, X. Tan, J. Lian, IR and XPS investigation of visible-light photocatalysis-nitrogen–carbon-doped TiO_2 film, Appl. Surf. Sci. 253 (2006) 1988–1994.
[30] T. Sano, N. Negishi, K. Koike, K. Takeuchi, S. Matsuzawa, J. Mater. Chem. 14 (2004) 380–384.
[31] H. Irie, Y. Watanabe, K. Hashimoto, Nitrogen-concentration dependence on photocatalytic activity of $TiO_{2-x}N_x$ powders, J. Phys. Chem. B 107 (2003) 5483–5486.
[32] I. Ilisz, A. Dombi, Investigation of the photodecomposition of phenol in near-UV irradiated aqueous suspensions II. Effect of charge-trapping species on product distribution, Appl. Catal. A 180 (1999) 35–45.
[33] A. Sobczynski, L. Duczmal, W. Zmudzinski, Phenol destruction by photocatalysis on TiO_2: an attempt to solve the reaction mechanism, J. Mol. Catal. A 213 (2004) 225–230.
[34] C.B. Almquist, P. Biswas, Role of synthesis method and particle size of nanostructured TiO_2 on its photoactivity, J. Catal. 212 (2002) 145–156.
[35] N.R.C. Fernandez Machado, V.S. Santana, Influence of thermal treatment on the structure of and photocatalytic activity of TiO_2 P25, Catal. Today 107/108 (2005) 595–601.
[36] J. Rengifo-Herrera, A. Mielczarski, E. Mielczarski, J. Castillo, N.C. Kiwi, J.C. Pulgarin, *E. coli* inactivation by N, S co-doped commercial TiO_2 powders under UV and visible light, Appl. Catal. B 84 (2008) 448–456.
[37] D. Mitoraj, A. Janczyk, M. Strus, H. Kisch, G. Stochel, P.B. Heczko, W. Macyk, Visible light inactivation of bacteria and fungi by modified titanium dioxide, Photochem. Photobiol. 6 (2007) 642–648.
[38] M. Mrowetz, W. Balcerski, A.J. Colussi, M.R. Hoffmann, Oxidative power of nitrogen-doped TiO_2 photocatalysts under visible illumination, J. Phys. Chem. B 108 (2004) 17263–17269.
[39] S. Livraghi, M.C. Paganini, E. Giamello, A. Selloni, C. Di Valentin, G. Pacchioni, Origin of photoactivity of nitrogen-doped titanium dioxide under visible light, J. Am. Chem. Soc. 128 (2006) 15666–15671.
[40] T. Tachikawa, S. Tojo, K. Kawai, M. Endo, M. Fujitsuka, T. Ohno, K. Nishijima, Z. Miyamoto, T. Majima, Photocatalytic oxidation reactivity of holes in the sulfur- and carbon-doped TiO_2 powders studied by time-resolved diffuse reflectance spectroscopy, J. Phys. Chem. B 108 (2004) 19299–19306.
[41] J.A. Rengifo-Herrera, K. Pierzchala, A. Sienkiewicz, L. Forró, J. Kiwi, C. Pulgarin, Abatement of organics and E. coli by N, S co-doped under UV and UV–vis light. Implications of the formation of singlet oxygen ($^1O_2$) under visible light, Appl. Catal. B. 88 (2009) 398–406.
[42] Z. Cheng, Y. Li, What is responsible for the initiating chemistry of iron-mediated lipid peroxidation: an update, Chem. Rev. 107 (2007) 748–766.
[43] T. Hirakawa, T. Daimon, M. Kitazawa, N. Ohguri, C. Koga, N. Negishi, S. Matsuzawa, Y. Nosaka, An approach to estimating photocatalytic activity of TiO_2 suspension by monitoring dissolved oxygen and superoxide ion on decomposing organic compounds, J. Photochem. Photobiol. A 190 (2007) 58–68.
[44] D. Sawyer, J.S. Valentine, How super is superoxide? Acc. Chem. Res. 14 (1981) 393–400.
[45] T. Daimon, T. Hirakawa, M. Kitazawa, J. Suetake, Y. Nosaka, Formation of singlet molecular oxygen associated with the formation of superoxide radicals in aqueous suspensions of TiO_2 photocatalysts, Appl. Catal. A 340 (2008) 169–175.